Supplementary Appendix

This appendix has been provided by the authors to give readers additional information about their work.

Supplement to: McDonough JE, Yuan R, Suzuki M, et al. Small-airway obstruction and emphysema in chronic obstructive pulmonary disease. N Engl J Med 2011;365:1567-75.

The relationship between small airway obstruction and emphysema in COPD - Online Supplement

Table of Contents

Online Supplement 1: Disector method of counting airways on MDCT

Stereology provides a method of quantifying irregularly shaped 3-dimensional objects from 2-dimensional profiles using test probes (i.e. lines, points, etc). Typically these methods are biased due to assumptions concerning the size and shape of the objects being measured. The Disector principle provides an unbiased sampling technique used to estimate the number of objects within a given volume defined by two sections separated by a known distance. These sections can either be separate histological sections known as a physical disector, or by focusing through a tissue sections known as an optical disector. In this study a variation on the optical disector method was used for the HRCT and microCT analyses of the lung tissue which we describe as a CT disector. The principles of the disector involve identifying the object on one section and seeing if the object continues onto the second (i.e. lookup) section. If this object is found on both sections it is excluded from the count, otherwise it is counted. From these counts and the 3-dimensional volume (defined as the area of the section and the distance between them), a density of object is determined which can be calculated to an absolute number by the reference volume of the whole structure being measured, e.g. the whole lung. More detailed descriptions can be found in Sterio[1], Howard and Reed[2], and Hsia *et al*.[3]

Figure 1S: An example of 3 discrete objects (A, B, C) intersecting with a defined reference volume of space. Object A passes through both the upper and lower surface of the volume. Object B passes only through the lower surface defined as the look-down plane and object C only through the upper surface defined as the look-up plane. When comparing two planes for counting an object, object A would be excluded from the count as it is present on both planes. Object B would only be counted when comparing the plane of interest with its look-up plane. Object C would only be counted when comparing its plane of interest with its look-down plane.

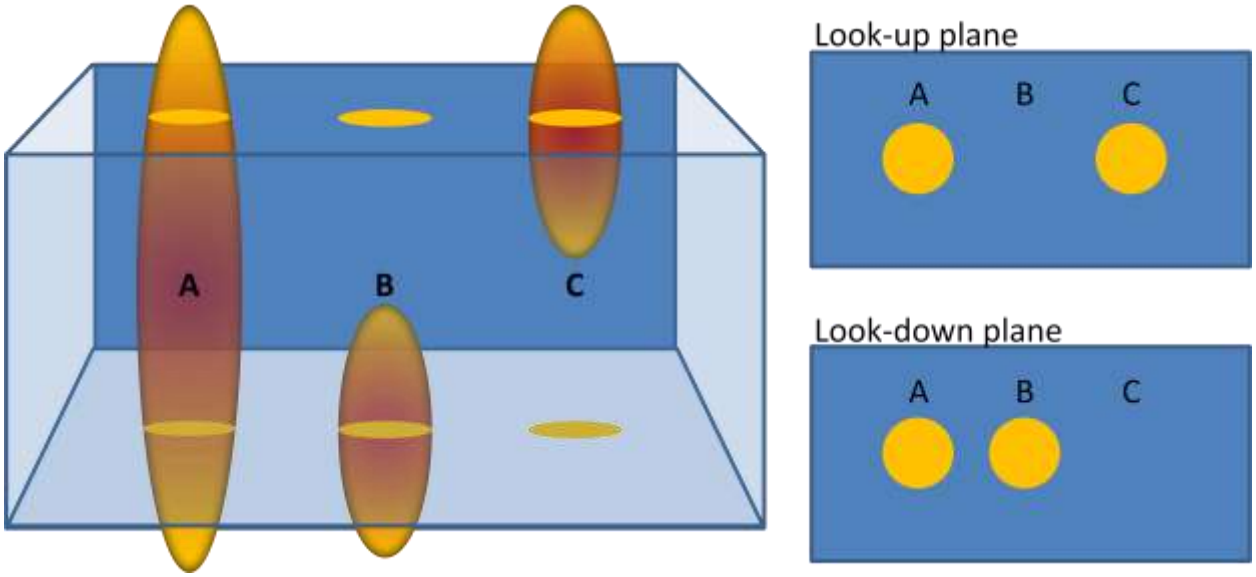

Figure 2S: An example of a pair of MDCT images analyzed using the Disector method. The airway of interest (arrow) show 2 airways counted in the lookup plane become one airway in the lookdown plane. Therefore, counting in both the lookup and lookdown directions account for both mother and 2 daughter branches of airways that divide within the reference frame, without violating the principle that only airways present in one plane and not the other are counted when calculating the number of airways within the lung.

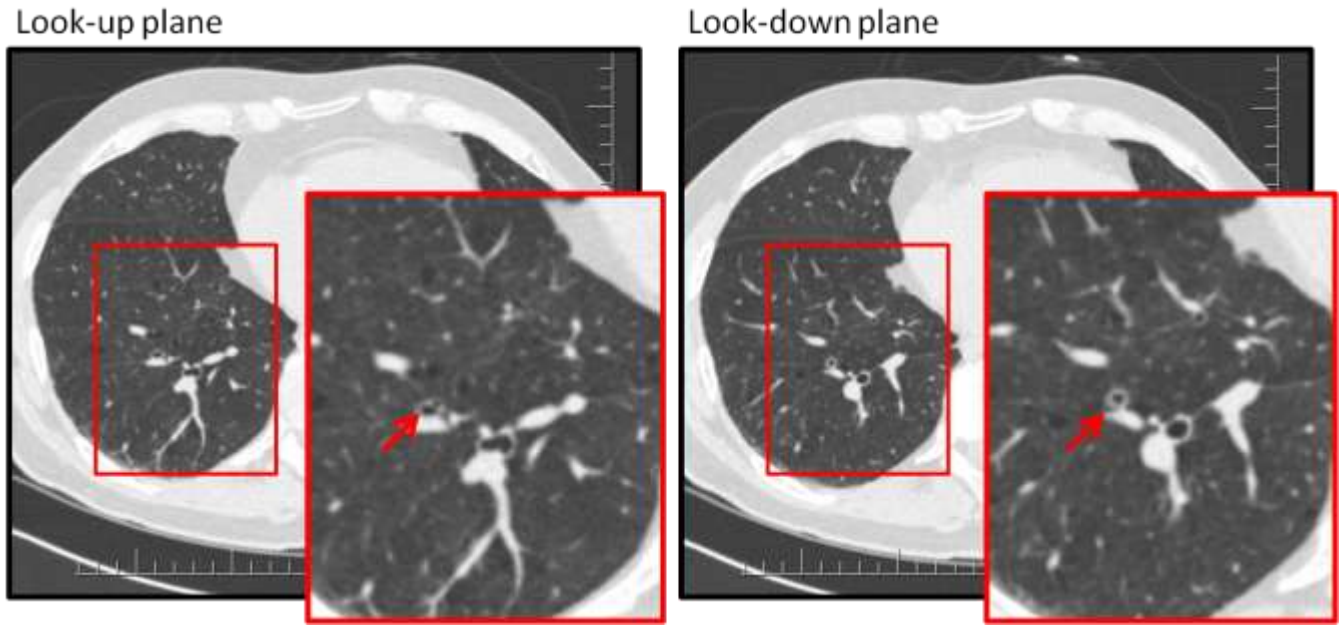

Online Supplement 2: Determining small airway number in each generation of branching

The visible airways in each generation of branching were determined from the MDCT scans of 4 control, 4 CLE, and 4 PLE lungs specimens. Software (ImageJ, NIH Bethesda, MD) was used to follow each pathway from the main stem bronchus to the periphery of the lung. The bifurcation at the terminus of the airway defined the division from one generation to the next and the total numbers of airways counted in each generation were summed to determine the number of branches in each generation. In addition, airway location was recorded to keep track of whether the airways branched into the upper or lower lobes of the lung.

These data were then compared to published data from airway casts (main manuscript: figure 2B). They show that in control lungs airways down to 2.5 mm in diameter were included in the count. Therefore, we conclude 2.5 mm to be the minimum size of airways which can be resolved by reconstructing the airways from MDCT using this specific protocol of counting terminal bifurcations. This is with the caveat that airways smaller than 2.5 mm diameter are still visible on MDCT images but any bifurcation at their terminus is below the resolution of the CT image. In contrast to the control lungs, the reconstruction of the bronchial tree of lungs from patients with the PLE phenotype of COPD showed a sharp reduction and leftward shift of the distribution of airways and those with the CLE phenotype showed an even sharper reduction in the airways smaller than 3 mm in diameter.

Online Supplement 3: Obtaining a representative sample of lung for microCT

Figure 3S: Compares the frequency distribution of voxel density in Hounsfield units for the entire lung to the frequency distribution of the Hounsfield units measured in the sampled sites of these lungs (see figure 1 of the manuscript for a description of how these sites were located). These data show that for the 4 cases of the CLE phenotype of COPD and 4 control cases, the frequency distribution of all the voxels in the lung and the frequency distribution of the voxels in the sample sites are not different from each other (P > 0.05). These data provide direct evidence that the sample sites used for the microCT studies are representative of the entire lung.

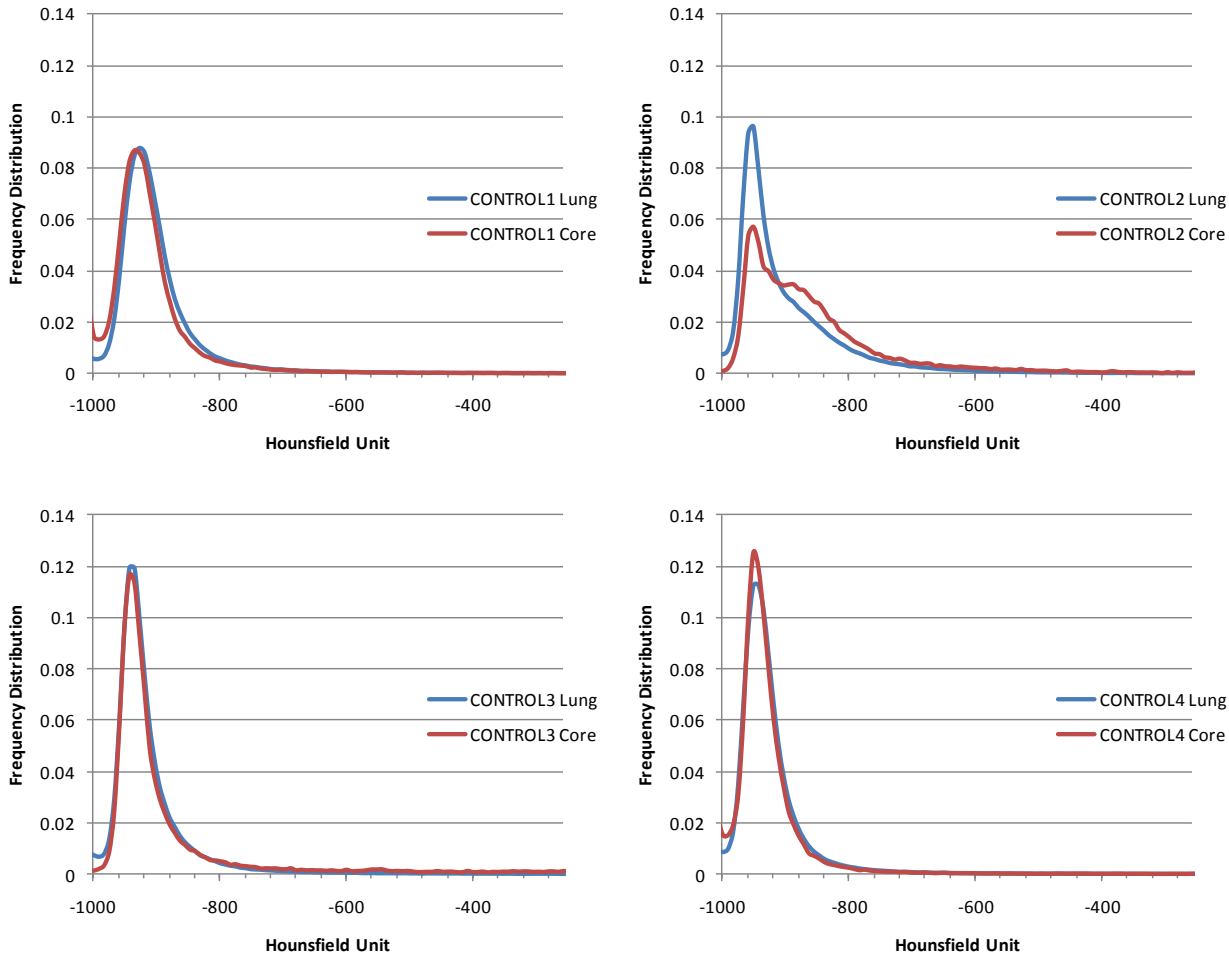

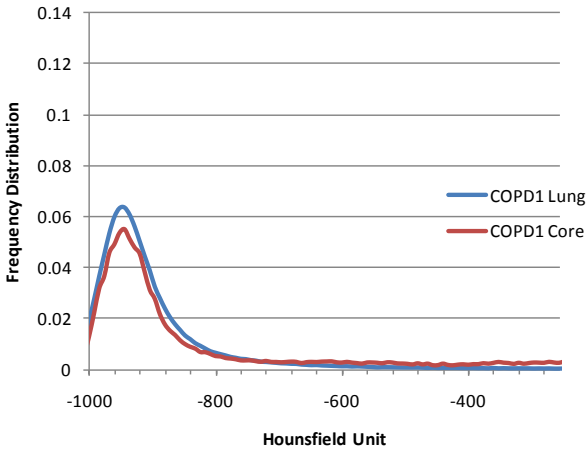
0.14
0.12
0.1
0.08
0.06
0.04
0.02
0
-1000
-800
-600
-400
Frequency Distribution
Hounsfield Unit
COPD1 Lung
COPD1 Core

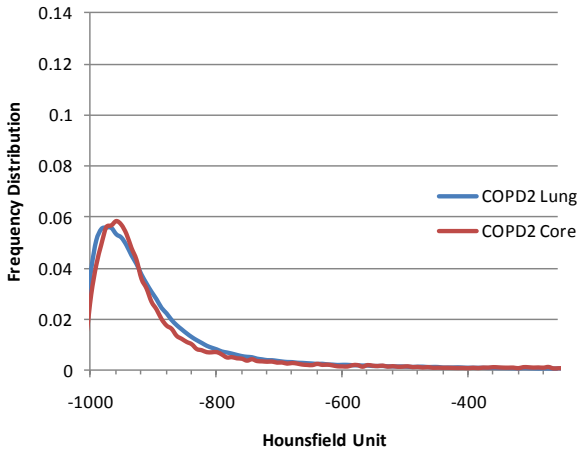
0.14
0.12
0.1
0.08
0.06
0.04
0.02
0
-1000
-800
-600
-400
Frequency Distribution
Hounsfield Unit
COPD2 Lung
COPD2 Core

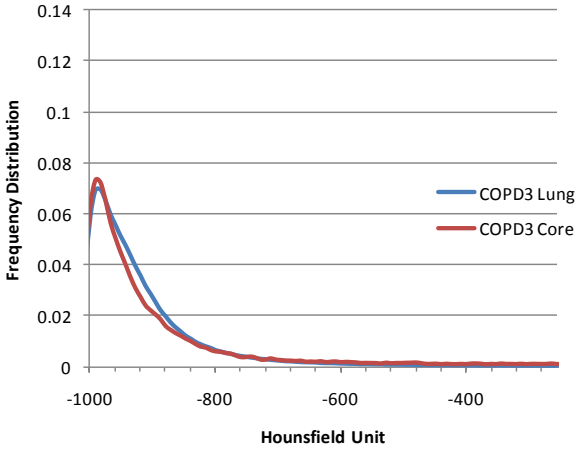
0.14
0.12
0.1
0.08
0.06
0.04
0.02
0
-1000
-800
-600
-400
Frequency Distribution
Hounsfield Unit
COPD3 Lung
COPD3 Core

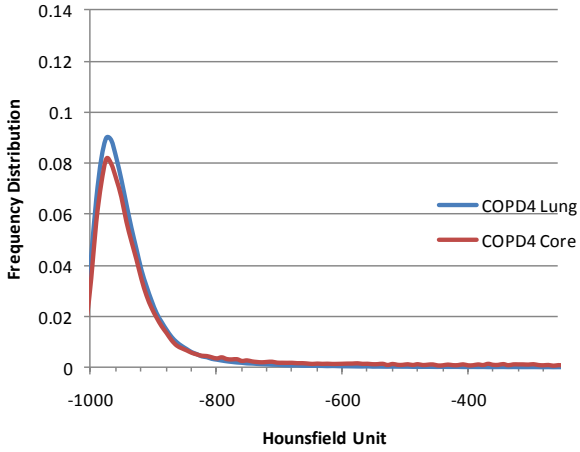
0.14
0.12
0.1
0.08
0.06
0.04
0.02
0
-1000
-800
-600
-400
Frequency Distribution
Hounsfield Unit
COPD4 Lung
COPD4 Core

Online Supplement 4: MicroCT image of a terminal bronchiole in COPD

Figure 4S: MicroCT images of serial cross-sectional cuts of a single terminal bronchiole from a patient with COPD. Note that the lumen progressively narrows in serial sections 1-3 and then progressively increases in size in sections 4 and 5 until it opens into the respiratory bronchiole in the section 6. Additional supplemental videos are included to illustrate the narrowing of the terminal bronchiole lumen in an airway from a COPD subject (see video file "COPD Lung Terminal Bronchiole": bottom-left) and a normal terminal bronchiole lumen in an airway from a control subject (see video file "Control Lung Terminal Bronchiole": bottom).

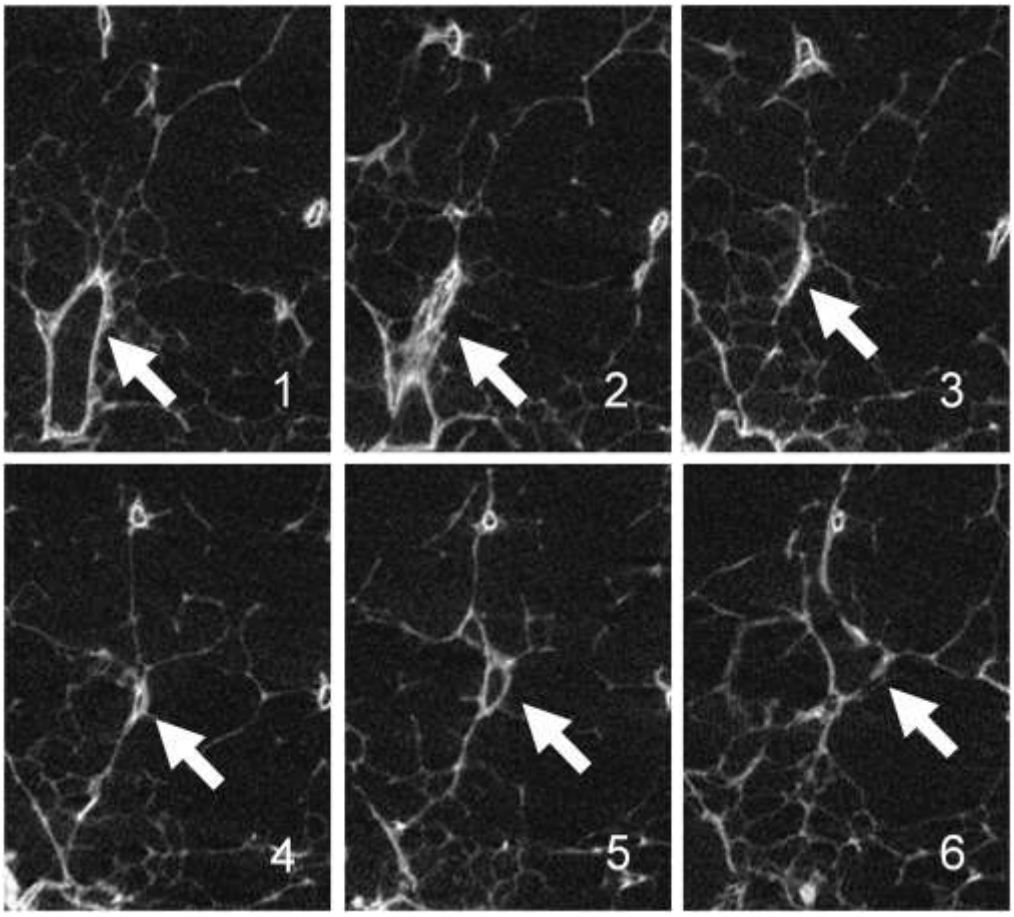

Online Supplement 5: Comparison of microCT to histological images

Figure 5S: A) (clockwise from top-left) Shows a cut surface of the tissue core that had been scanned for microCT before it was cut. A reconstruction from the microCT scan at the same level the cut was made. A single slice from the microCT image stack showing the tissue surface. A histological section cut at the same tissue level after the core was embedded in JB4 showing the tissue surface. Note the flap of tissue is seen to contain a vessel on the thick sections of tissue (arrow) and that this 3-dimensional structure becomes a 2-dimensional line on the single microCT image and histological section. B) A high degree of correlation was found for Lm measurements made on histological sections of JB4 embedded samples and microCT sections. Comparison of the Lm measurement showed R-squared = 0.8323 and slope of 0.9469 when intercept was set at y = 0.

A

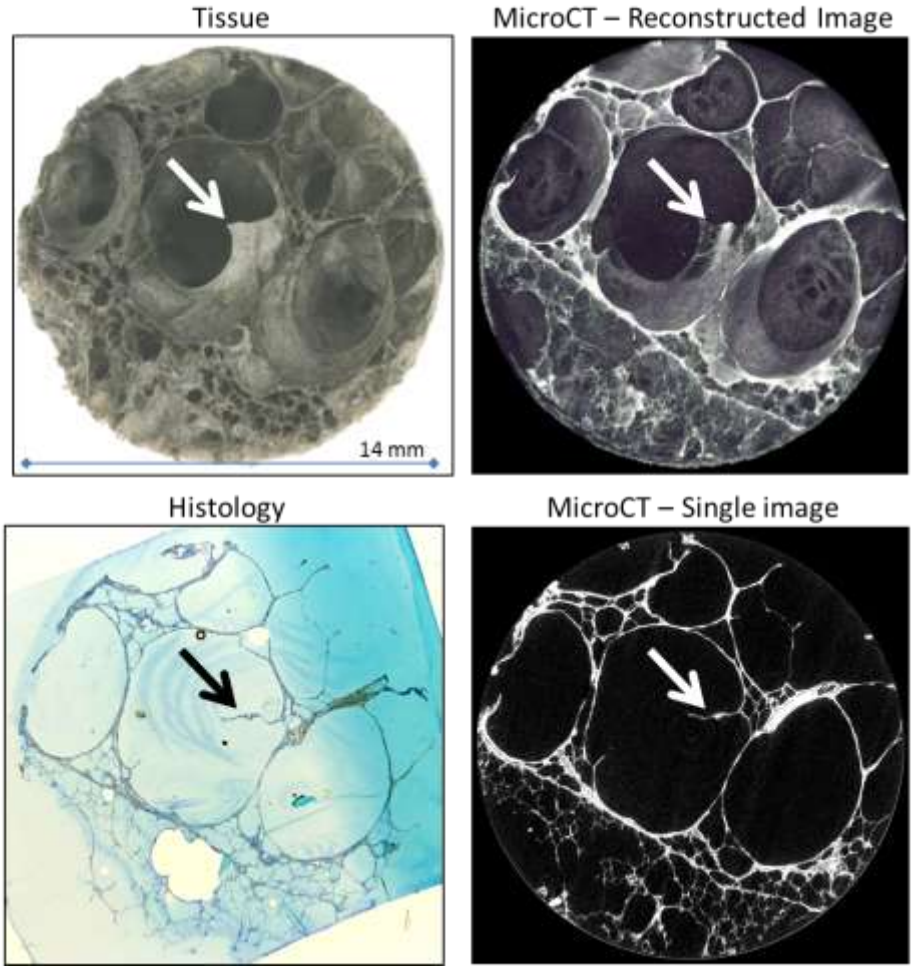
Tissue
MicroCT – Reconstructed Image
14 mm
Histology
MicroCT – Single image

B

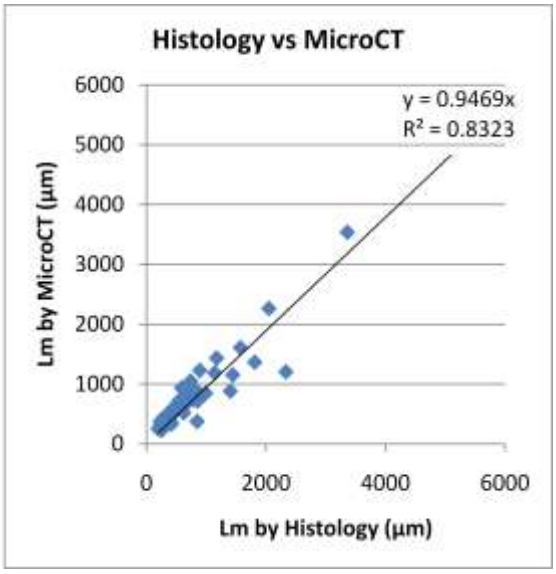
Histology vs MicroCT
y = 0.9469x
R² = 0.8323
Lm by MicroCT (µm)
Lm by Histology (µm)
0
1000
2000
3000
4000
5000
6000
0
2000
4000
6000

Online Supplement 6: Counting airways by histology and microCT

Figure 6S: Compares the number of terminal bronchioles/mL lung obtained by microCT examination of the entire tissue core to the number obtained using histological sections cut from JB4 embedded tissue from the same tissue cores to construct a physical disector. The physical disector method examined the volume of tissue between two sections cut 0.72 mm apart, with cross-sectional areas of 1 cm^2 and a total disector volume of 0.072 mL. The average number of airways present on the lookup and lookdown sections were counted and compared to matched microCT images using the same criteria for both datasets (physical disector method). In practice, this comparison was restricted to control subjects as there were two few airways in the diseased lung tissue to count using histology based methods. Although there was a trend for the histology based method to count fewer airways/mL, the difference between the two methods was not significant (P = 0.28).

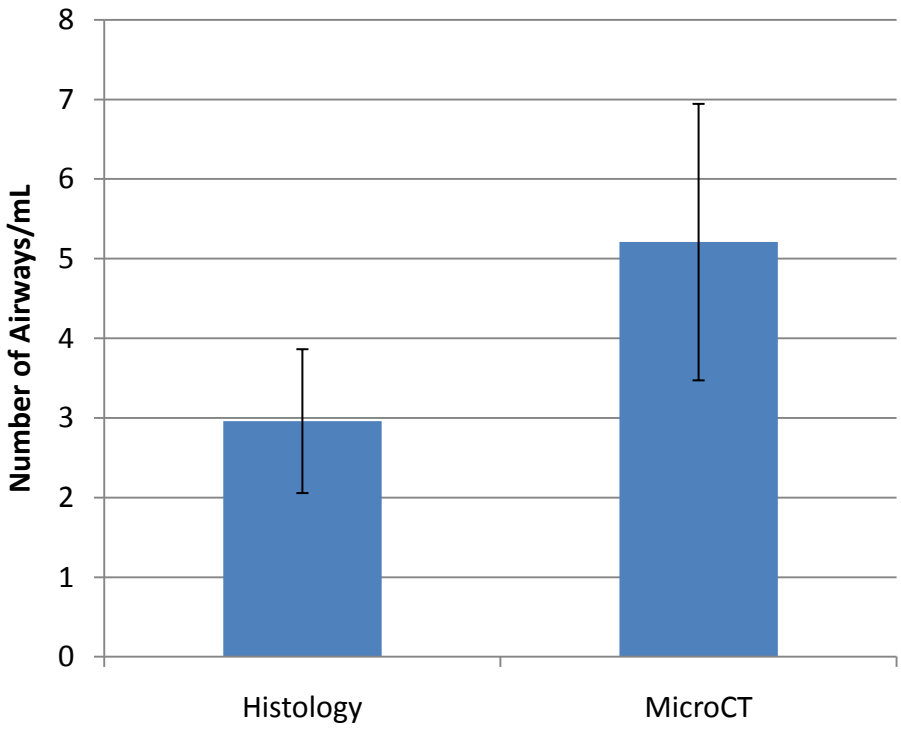

Online Supplement 7: Intra and interobserver comparison of airway counts in MDCT and microCT

Intra and interobserver comparisons confirmed that the counting techniques used are reproducible. Figure 7S shows a strong correlation (R-squared = 0.80) between data obtained by the same observer's measurements of airways/lung pair obtained by comparing lookup to lookdown sections to measurements in the inverse direction of comparing lookdown to lookup sections. Figure 8S shows a similarly strong correlation (R-squared = 0.76) between observations made by a second observer on 20 of the 78 cases examined by the first observer.

Figure 7S: Intraobserver measurements for airway counts on the 78 subjects using MDCT.

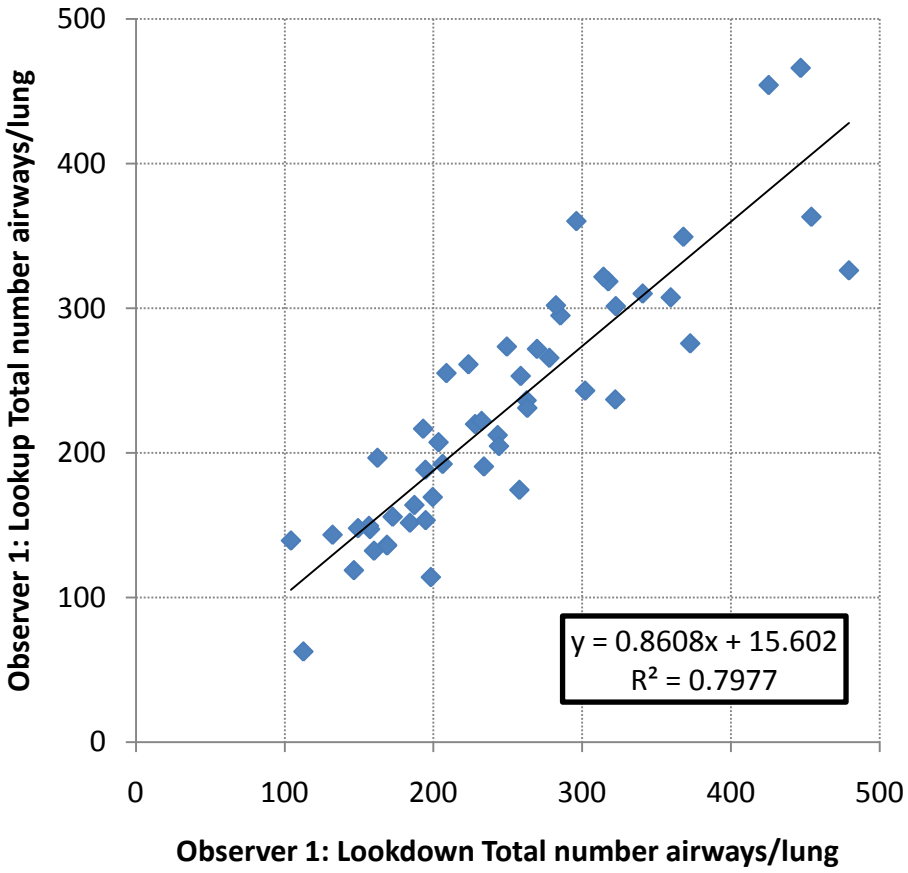

Figure 8S: Interobserver measurements for airway counts on a subset (20) of the 78 subjects using MDCT.

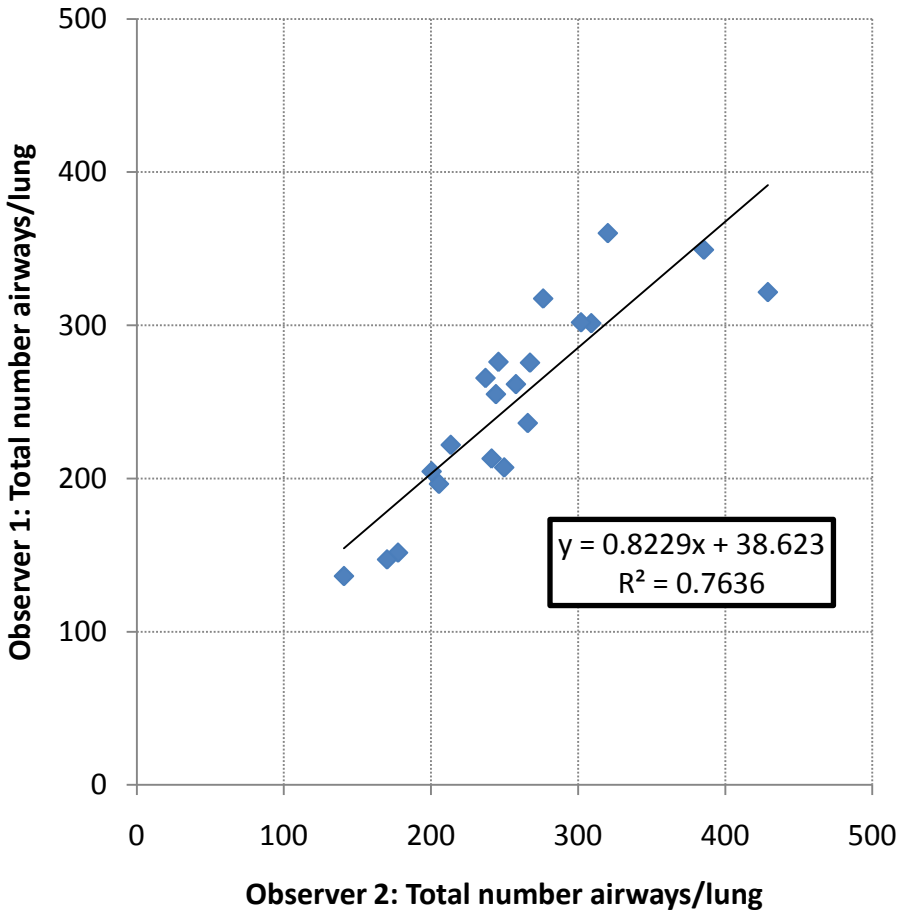

Figure 9S: Shows a relatively strong correlation (R-squared = 0.75) between the number of airways counted by two separate observers that followed the airways from the bronchus to their terminus and counting the number of airway bifurcations per generation from MDCT images of isolated lungs.

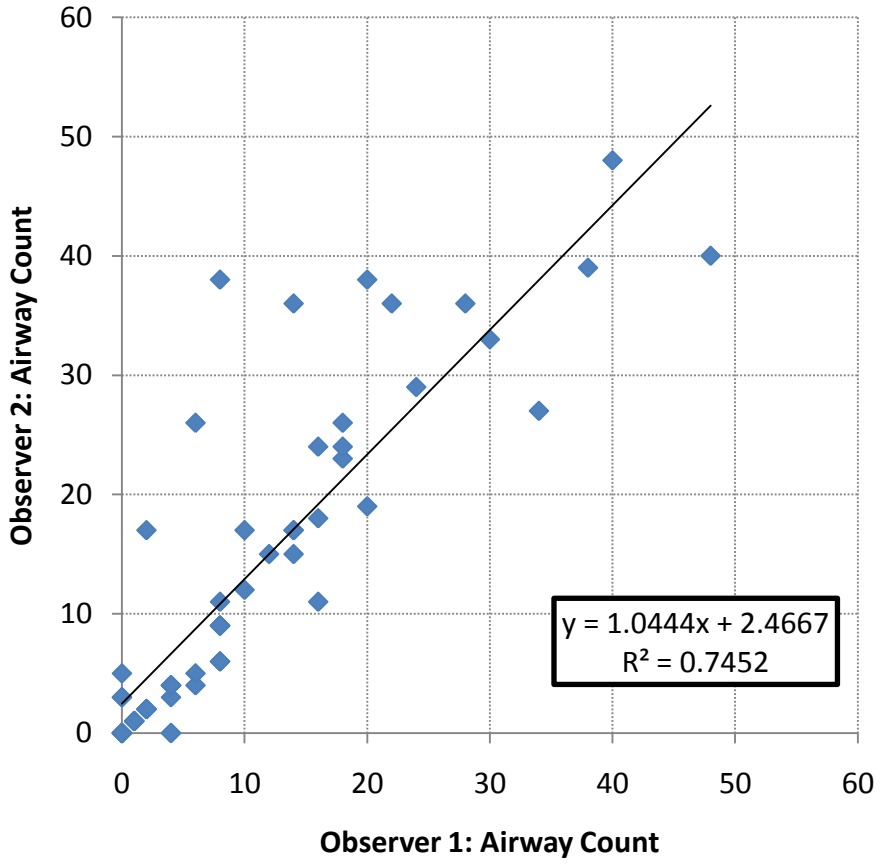

Figure 10S: Shows a similarly strong correlation (R-squared = 0.79) between 2 observers that counted the number of terminal bronchioles per lung tissue core from the microCT scans.

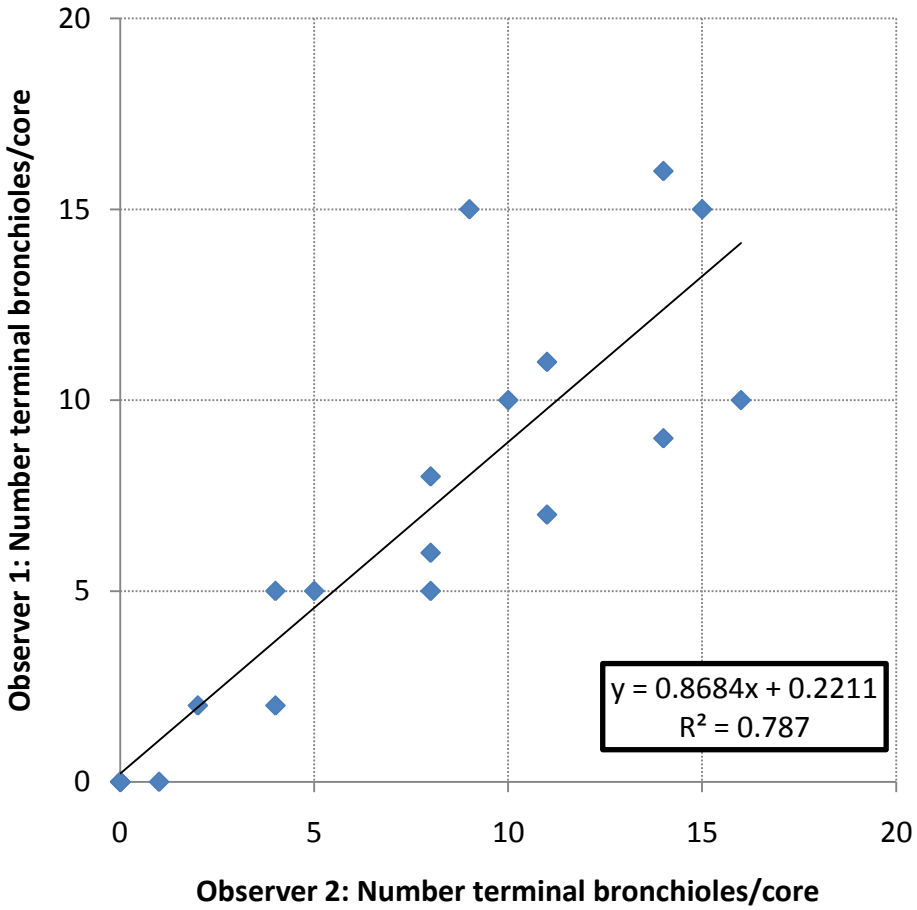

Online Supplement 8: Terminal bronchiole number and dimensions compared to previous studies

Figure 11S: Shows that the present data on terminal bronchiole diameter (A), and cross-sectional area (B) obtained from microCT images of our control subjects closely match those previously reported by Weibel.[4,5] Moreover, the numbers of terminal bronchioles/lung pair obtained in this study (44,510±15,574; Mean±S.D.) closely matches the mean of four previous studies from casts (44,500±18,574) of normal human lungs[4,6-8] summarized in table 3 by Horsfield and Cumming.[8]

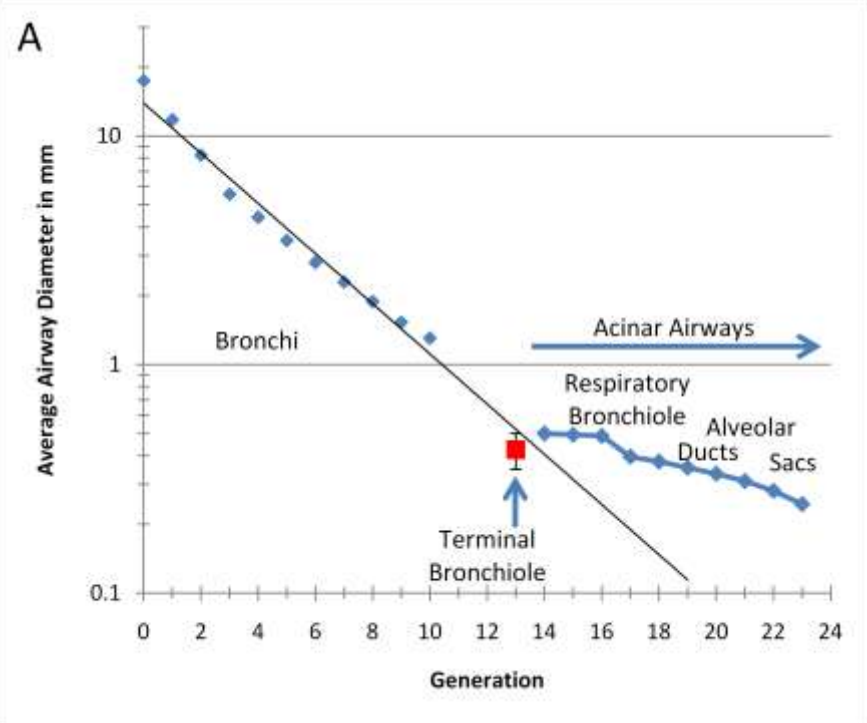
A
Average Airway Diameter in mm
10
1
0.1
Bronchi
Acinar Airways
Respiratory
Bronchiole
Alveolar
Ducts
Sacs
Terminal
Bronchiole
0 2 4 6 8 10 12 14 16 18 20 22 24
Generation

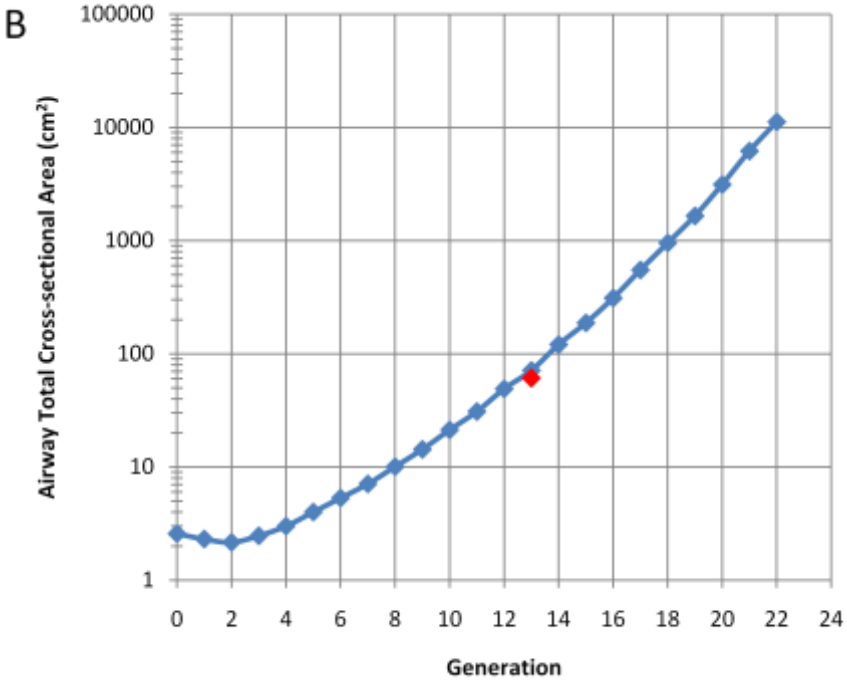
B
Airway Total Cross-sectional Area (cm²)
100000
10000
1000
100
10
1
0 2 4 6 8 10 12 14 16 18 20 22 24
Generation

Online Supplement 9: Branching of airways into the upper and lower lung

Figure 12S: Summarizes the HRCT data concerning the number of airways in each generation branching into either the upper (A) or lower (B) regions of individual lungs from control (N=4), CLE (N=4), and PLE (N=4) cases. Comparison of the control lungs to lungs affected by PLE shows no difference in the upper lung region and a sharp reduction in the lower lung regions where PLE causes greater emphysematous destruction (see figure 3B in main manuscript). In contrast, comparison of the control lungs to the lungs affected by CLE show a sharp reduction in both upper and lower regions of the lung even though CLE causes greater destruction of the upper lung region (see figure 3A in main manuscript). These HRCT data are consistent with the microCT data (figure 3D) showing a much greater reduction in terminal bronchioles in non-emphysematous regions (i.e. ≤ 489 μm) in lungs from patients with CLE than lungs affected by PLE.

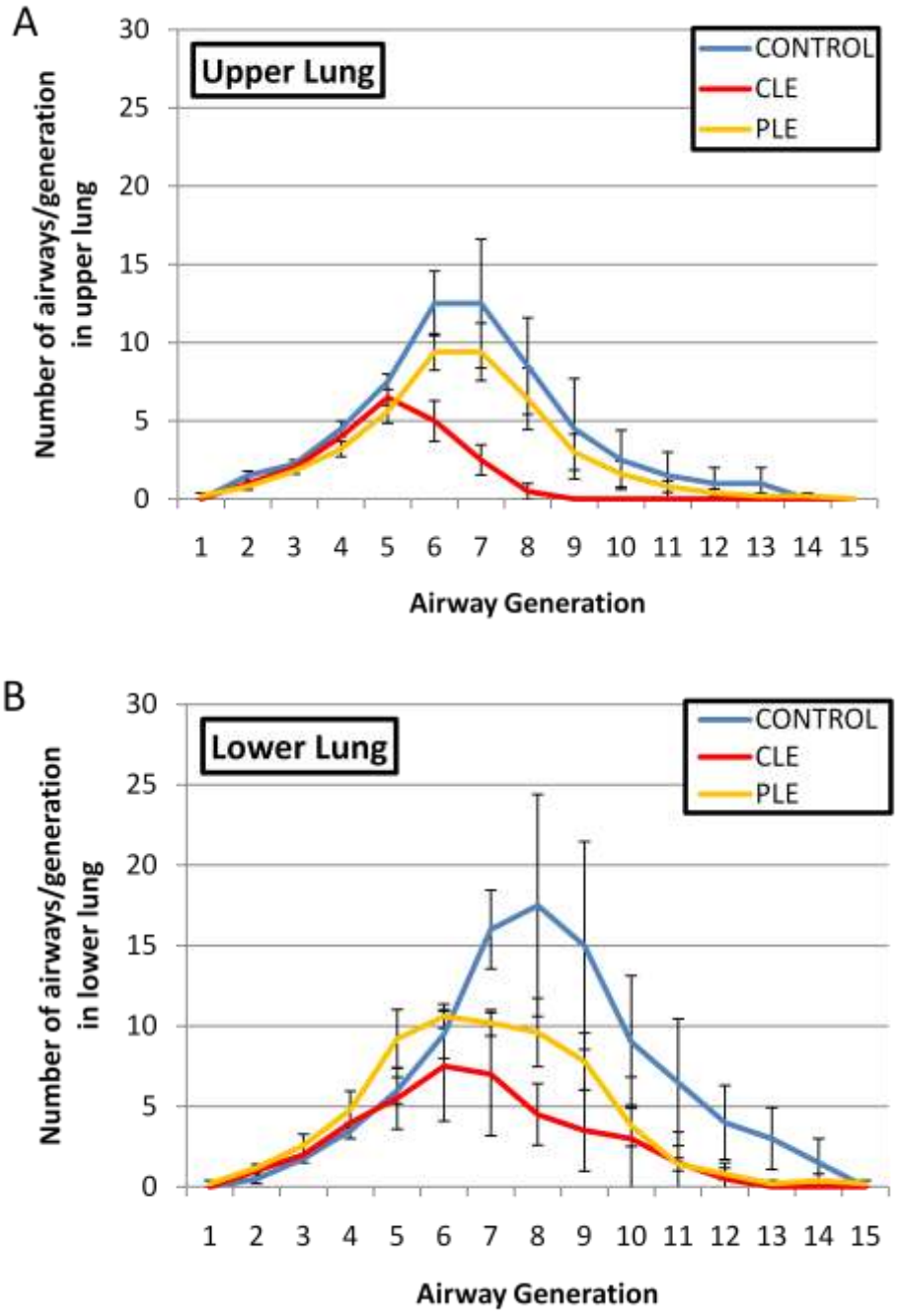
A
Upper Lung
CONTROL
CLE
PLE
Number of airways/generation in upper lung
30
25
20
15
10
5
0
1 2 3 4 5 6 7 8 9 10 11 12 13 14 15
Airway Generation
B
Lower Lung
CONTROL
CLE
PLE
Number of airways/generation in lower lung
30
25
20
15
10
5
0
1 2 3 4 5 6 7 8 9 10 11 12 13 14 15
Airway Generation

Online Supplement 10: A shift to smaller diameter airways in COPD lungs

Figure 13S: Comparison of data from Matsuba and Thurlbeck[9] and Bignon *et al*.[10] to the present results shows that all three studies reported a left-shift in the small airway diameters in diseased lungs compared to controls. However, the results reported here (table 1B, main manuscript) extend this finding by showing an 81-99.7% reduction in total lumen area and 72-89% reduction in number of terminal bronchioles that readily explain the 4-40 fold increase in small airway resistance measured in COPD.

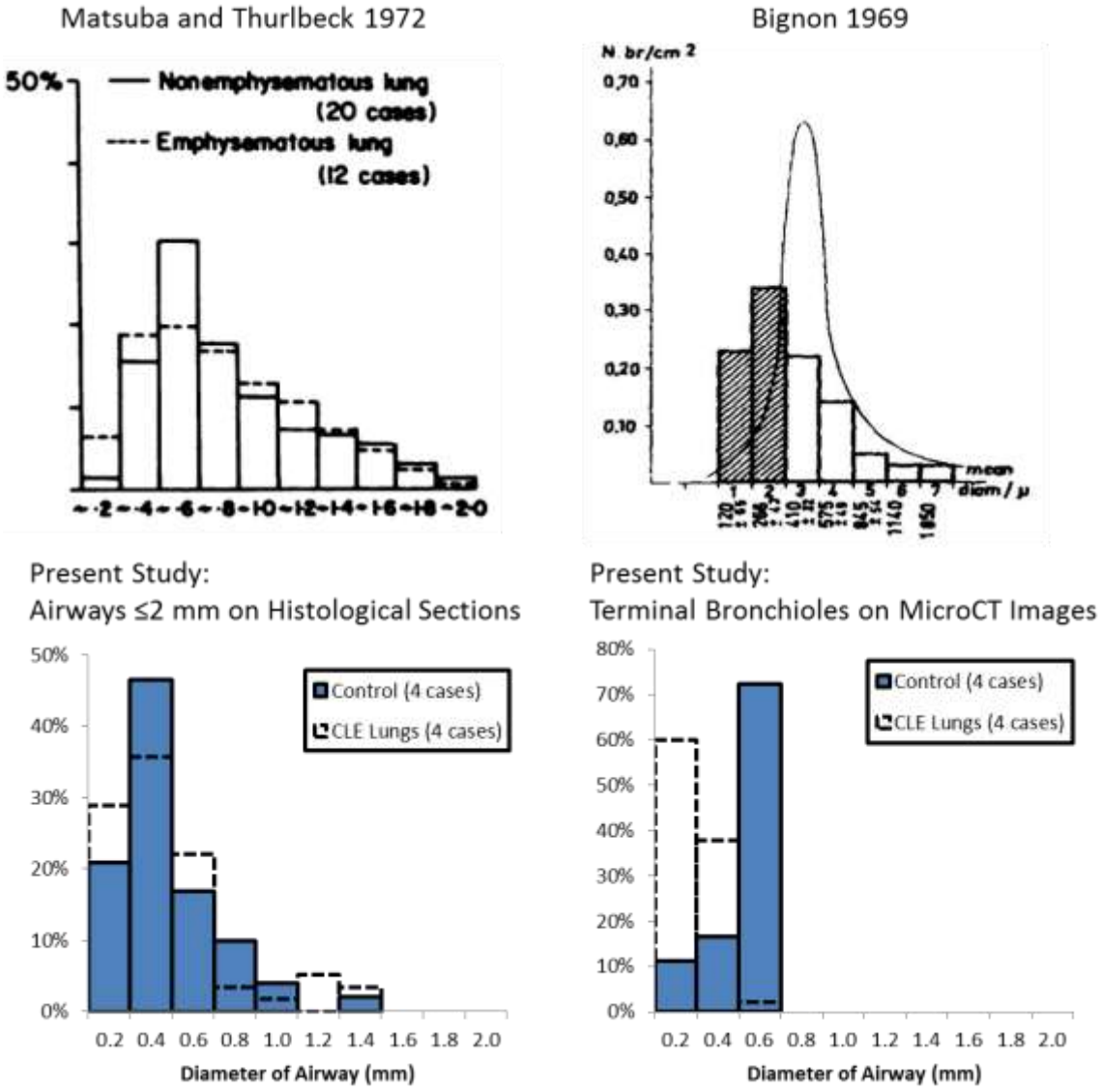

References:

1. Sterio DC. The unbiased estimation of number and sizes of arbitrary particles using the disector. J Microsc 1984;134:127-36.
2. Howard CV, Reed MG. Unbiased Stereology: Three-Dimensional Measurement in Microscopy. Oxford, UK: BIOS Scientific Publishers Ltd; 1998.
3. Hsia CC, Hyde DM, Ochs M, Weibel ER. An official research policy statement of the American Thoracic Society/European Respiratory Society: standards for quantitative assessment of lung structure. Am J Respir Crit Care Med 2010;181:394-418.
4. Weibel ER. Morphometry of the Human Lung. New York: Academic Press Inc; 1963.
5. Weibel ER. What makes a good lung? Swiss Med Wkly 2009;139:375-86.
6. Rohrer F. Der Stromungswiderstand in der menschlichen Atemwegen und der Einfluss der unregelmässigen Verzweigung es Bronchial-systems auf der Atmungsverlauf in vershiedenen Lungenbezinken. Arch Ges Physiol 1915;162:225-9.
7. Findeisen W. Uber das Absetzen kleiner, in dur Luft suspendierter Teilchen in der menschlichen Lunge bei der Atmung. Arch Ges Physiol 1935;236:367-79.
8. Horsfield K, Cumming G. Morphology of the bronchial tree in man. J Appl Physiol 1968;24:373-83.
9. Matsuba K, Thurlbeck WM. The number and dimensions of small airways in emphysematous lungs. Am J Pathol 1972;67:265-75.
10. Bignon J, Khoury F, Even P, Andre J, Brouet G. Morphometric study in chronic obstructive bronchopulmonary disease. Pathologic, clinical, and physiologic correlations. Am Rev Respir Dis 1969;99:669-95.